Strong Coupling of Nonlinear Electronic and Biological Oscillators: Reaching the "Amplitude Death" Regime

I. Ozden,[1] S. Venkataramani,[1] M. A. Long,[3] B.W. Connors,[3] and A.V. Nurmikko[1,2,*]

[1]*Department of Physics, Brown University, Providence, Rhode Island 02912, USA*

[2]*Division of Engineering, Brown University, Providence, Rhode Island 02912, USA*

[3]*Department of Neuroscience, Brown University, Providence, Rhode Island 02912, USA*

(Received 29 January 2004; published 4 October 2004)

Interaction between an electronic and a biological circuit has been investigated for a pair of electrically connected nonlinear oscillators, with a spontaneously oscillating olivary neuron as the single-cell biological element. By varying the coupling strength between the oscillators, we observe a range of behaviors predicted by model calculations, including a reversible low-energy dissipation "amplitude death" where the oscillations in the coupled system cease entirely.

DOI: 10.1103/PhysRevLett.93.158102 PACS numbers: 87.68.+z, 87.16.Xa

The creation of bidirectional communication interfaces between man-made and biological systems is being sought by a broad spectrum of approaches. In case of neural circuits, these range from attempts to develop systems level "neuroports" at the brain-machine interface to research at the cellular level of individual neurons. The study of these interfaces aims to understand the functional intricacies of neurons as biological information processors, but also to explore future approaches to electronic computers.

Here we report on experiment and theory of a particular neural-electronic hybrid interface forming a system of coupled nonlinear oscillators. Coupled nonlinear oscillators are frequently studied in electrical engineering, physics, and computational biology, and applications are found, e.g., in superconducting junctions, phase-locked laser arrays, and relativistic magnetrons. Paired nonlinear oscillators show qualitatively different behavior depending on the coupling strength. In the weak coupling regime, oscillators either synchronize at a common frequency or behave independently. In the strong coupling regime, the oscillators can quench each other by dynamically pulling each other away from the oscillatory state to enter a nondissipative, zero-amplitude standstill, i.e., "amplitude death." In electronic circuits, recent work has demonstrated the existence of spontaneous amplitude death [1] as one striking illustration of the diverse possible phenomena predicted for such interactive systems [2]. In neuroscience, the electronic-neural cell hybrid systems have been used to study collective behavior of neural oscillators, such as central pattern generators [3]. In this work, we have been able to create an active interface between an electronic and neural oscillator circuit in the laboratory that dramatically reaches the amplitude death regime. As far as we know, this is the first demonstration of amplitude death in a biological system. Possible impact on neuroscience derives from intense current interest in developing ways to control neuropathological behaviors with electronic devices that can deliver stimuli at the precise time and place, and with the appropriate pattern, to prevent or terminate deleterious neural activity.

Our biological circuit element was a neuron from the inferior olivary (IO) nucleus of the rat brain. IO cells exhibit spontaneous oscillations in their membrane potential, with typical amplitudes of 0.1–15 mV in the range of 1–10 Hz. Neurons of the IO are the source of the climbing fibers to the cerebellar cortex, and they strongly excite Purkinje cells. This circuit is believed to be a critical feature of precise timing and learning in cerebellar motor circuits. Studies of the IO have revealed many details of their physiological mechanisms [4]. These neurons are coupled to one another by electrical synapses which enable synchrony of membrane potential oscillations and action potentials across groups of cells in the IO [5,6]. However, experiments show that the oscillations themselves arise from the intrinsic membrane properties of individual cells [5], although electrical coupling may also play a role [7]. To simulate the nonlinear oscillatory behavior of IO neurons, we employed a variation of the model of Manor *et al.* [8] which uses Hodgkin-Huxley formalism [9]. It is known that a low-threshold calcium current is necessary for the oscillations in the IO which, together with a passive leakage current, leads to the following equations of motion:

$$\frac{dV}{dt} = -\frac{1}{C_m}(I_{\text{ion}} - I_{\text{app}}), \tag{1a}$$

$$\frac{dh}{dt} = \frac{h_\infty(V) - h}{\tau_h(V)}, \tag{1b}$$

where V is the membrane potential, $C_m = 1\ \mu\text{F/cm}^2$ is the specific capacitance of the membrane, I_{app} is the applied current of external input into the cell, and I_{ion} is the sum of a low-threshold calcium current I_T and a leakage current I_L [10]. The inactivation function $h(V, t)$ is related to the membrane ionic conductances [9] with h_∞

and τ_h corresponding to the steady-state (membrane potential and conductance-dependent) inactivation and inactivation time constants, respectively. The relevant parameters have been measured on the IO cells in rats [8]. We have used numerical techniques to solve Eq. (1) for a single, isolated IO neuron to obtain its bifurcation diagram and to verify the existence of a well-defined region of limit cycle oscillations [8,11].

For the electronic oscillator (ELO), we chose a parallel *RLC* circuit with a nonlinear resistive element [1]. The circuit design [Fig. 1(a)] and the individual component values were chosen so as to produce limit cycle oscillations variable over the range of 0.5–20 Hz, with amplitudes in the range of 1.0–50 mV. The nonlinear element, a version of the so-called Chua diode [12], was constructed using diodes, operational amplifiers, and resistors, with a designed differential negative resistance tailored by using the circuit analysis software SPICE. The required large inductance (~ 1000 Henry) was implemented by using generalized impedance converters. Our limit cycle oscillator obeys the following equation of motion:

$$\dot{x} = y, \qquad \dot{y} = -\frac{f'(x)}{C} y - \omega_0^2 x, \tag{2}$$

where $x = V(t)$ is the voltage across the circuit, $y = dV/dt$, $f(V)$ the current component flowing through the nonlinear resistor, and $\omega_0^2 = (LC)^{-1}$. We used numerical techniques to solve Eq. (2) to verify that our ELO, too, had stable limit cycle behavior.

By combining Eqs. (1) and (2), we explored the phase space for the electrically coupled IO and electronic nonlinear oscillators. The equations for the coupled system can be written as

$$\frac{dV}{dt} = -\frac{1}{C_m}(I_{\text{ion}} + K_1[A(V - V_{\text{rest}}) - x]), \tag{3a}$$

$$\frac{dh}{dt} = \frac{h_\infty(V) - h}{\tau_h(V)}, \tag{3b}$$

$$\dot{x} = y, \tag{3c}$$

$$\dot{y} = \left(-\frac{f'(x)}{C} - \frac{K_2}{C}\right) y - \omega_0^2 x - K_2 \frac{A}{C_m} I_{\text{ion}}, \tag{3d}$$

where A is gain to match the amplitudes of oscillations in both systems for a fair coupling. The salient features of these simulations are first summarized in the bifurcation diagram of Fig. 2. To accommodate for the physically very different energy content of the neuron and the circuit oscillator, their electronic coupling was adjusted through two independent "potentiometers," labeled K_1 and K_2. In the bifurcation diagram, the axes are the normalized coupling coefficients K_1 in units of $10\ \text{M}\Omega/R_{K1}$ and K_2 in $5\ \text{k}\Omega/R_{K2}$. In the calculations, the frequencies of oscillations were 1.3 and 1.9 Hz for the IO and ELO, respectively, as in the experiment. Given a range of dis-

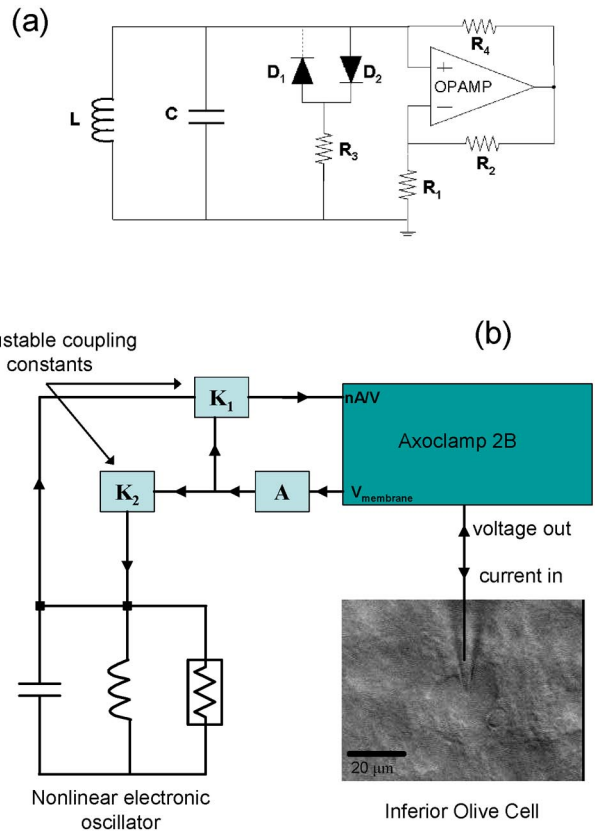

FIG. 1 (color online). (a) The electronic oscillator circuit with $R_1 = R_2 = 10\ \text{K}\Omega$, $R_3 = 35\ \text{K}\Omega$, $R_4 = 100\ \text{K}\Omega$, $C = 100$ nF, $L = 250\,000$ H. (b) Schematic of the experimental arrangement. The box A is an adjustable-gain amplifier to match the amplitudes of oscillations in electronic (typically 10–20 mV) and in biological (typically 5–15 mV) oscillators. Boxes K_1 and K_2 are also adjustable-gain amplifiers to determine different coupling coefficients.

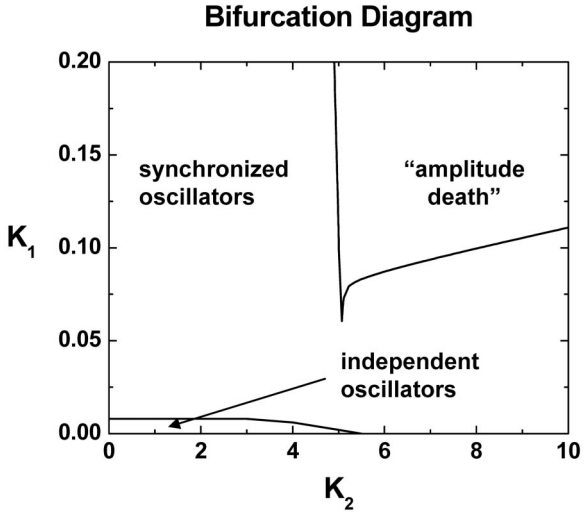

FIG. 2. Calculated bifurcation diagram for the coupled nonlinear olivary neuron-electronic oscillator pair, as a function of the coupling coefficients K_1 and K_2.

TABLE I. Experimental coupling coefficients.

	R_{K2}: IO to circuit	R_{K1}: Circuit to IO
Amplitude death	400 Ω	1 MΩ
In-phase oscillations	5 kΩ	70 MΩ
Out-of-phase oscillations	5 kΩ	100 MΩ

tributed oscillation frequencies and coupling strength between the two oscillators, the theory predicts the existence of a phase space for the coupled system that is sharply divided into three regions as a function of K_1 and K_2: (i) two independent oscillators ($K_1 = 0$, $K_2 = 0$), (ii) synchronized oscillators ($K_1 = 0.1$, $K_2 = 1$ for in-phase and $K_1 = 0.03$, $K_2 = 1$ for out-of-phase cases), and (iii) the case of "amplitude death" ($K_1 = 10$, $K_2 = 12$). Note that the amplitude death is exclusively a consequence of the nonlinear nature of the coupled oscillator problem in a *strongly interactive* regime and differs fundamentally from simple linear superposition phenomena such as interference.

Experimentally we constructed the coupled nonlinear oscillator circuit by connecting an IO neuron to our ELO through an electrical pathway, facilitated by a microelectrode connection to the neuron. Microelectrode interfaces have been utilized by neuroscientists to study the oscillatory properties of the IO neurons in detail, including work by Yarom and co-workers, who connected linear analog electrical circuits to IO neurons to investigate the relationship between intercellular coupling and synchronous membrane oscillations [13]. Our aim was to test the above predictions that arise from the theory of coupled nonlinear oscillator circuits. The bidirectional electrical connection to the olivary neuron was made through a whole-cell patch micropipette, connected to current in–voltage out amplifier-recording unit [14]. Slices from the IO from a rat's brain were prepared with a standard protocol [15]. With this arrangement, we studied the interaction between the two oscillators over a wide range of coupling conditions in steady state. Table I summarizes the values of the experimental coupling constants in each of the three regimes of Fig. 2. The key results of a successful run are summarized in Fig. 3. Figure 3(a) shows the oscillators acting independently in the weakly coupled regime (the IO also shows a single action potential spike, occasional phenomena not connected with issues studied here). With increasing coupling strength, the oscillators become phase locked, or synchronized at 1.7 Hz [Fig. 3(b)], but with a phase relationship which is either in phase or out of phase depending on the coupling parameters [Fig. 3(b), left vs right panels]. Finally, as shown in Fig. 3(c), further increasing the coupling strength results in amplitude death. That is, the active biological oscillator and the electronic circuit have the ability to extinguish their oscillations through their mutual interaction. As the coupling coefficients were next decreased in value, the oscillations recommenced; that is, the state of amplitude death was fully reversible. The results of the detailed computational solution to the coupled Eqs. (1) and (2), employing the technique developed by Ermentrout [2], are compared to the experiment in Figs. 3(d)–3(f), displaying close agreement.

We briefly comment on the physics of our coupled hybrid oscillator circuit in terms of the stability, noise,

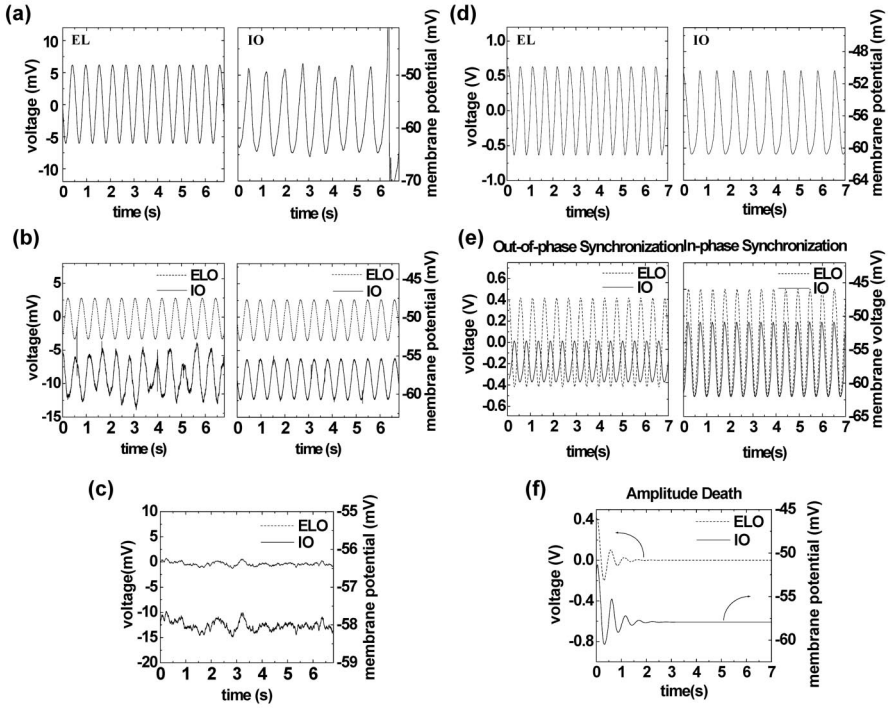

FIG. 3. (a)–(c) Experimental results for the coupled system in the weak coupling (independent oscillators), medium coupling (synchronous oscillation; in and out of phase), and strong coupling (amplitude death) regimes, respectively. (d)–(f) Corresponding results from theory in the three regimes; the amplitude death regime is reached after a transient following step function increase in the coupling coefficients.

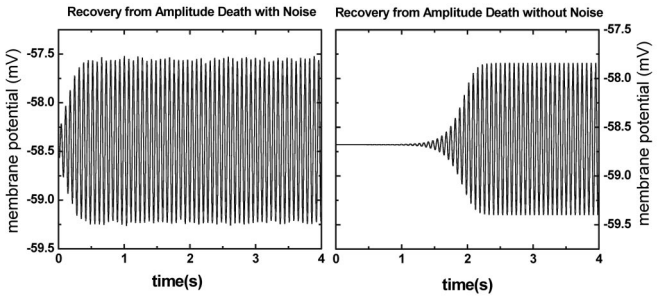

FIG. 4. Computed return from amplitude death in the presence and the absence of a 1 mV rms noise, respectively.

and dynamics of the quiescent amplitude death regime. All circuits are noisy at a finite temperature; for neural cells the primary noise generators are thermal noise of the membrane resistance, noise due to stochastic channel openings and closings of voltage-gated ion channels, and noise due to synaptic inputs from other neurons [16]. We highlight here the issue of the recovery of the system from the quiescent case, induced by the presence of a "white" noise spectrum applied as a Gaussian current input with zero mean in the term I_{app} of Eq. (1b). This results in a rms voltage noise of the membrane potential of approximately 1 mV. Figure 4 shows a comparison of the recovery from amplitude death of the system in the presence of noise and without noise. In principle, a noise-free system is not expected to recover from amplitude death; however, in this case it is hard to find the exact equilibrium point in simulations unless the computational time is extended to an impractical length. Nonetheless, it is clear from Fig. 4 that the presence of noise significantly accelerates the recovery rate, on the time scale of the average oscillation frequency. Details of the stochastic problem will be addressed elsewhere.

The combined experimental and theoretical results presented above represent a demonstration of strongly interactive, *real-time,* electronic-neural cell interface, where electronic and neural cells communicate *beyond the perturbative regime.* The demonstrated ability of the coupled system to cease its spontaneous oscillations in a reversible manner, as well as the synchronization of oscillations, represents a potentially powerful general concept where biological and man-made circuits can be envisioned to interact as a hybrid unit, with predesigned functional performance for the total "closed-loop" system. For neuroscience applications, the phenomenon of amplitude death suggests a dynamical strategy for rapidly and effectively terminating electronically a wide range of undesirable oscillatory behaviors, such as the control of abnormal tremors. Extension of this work envisions the study of the collective interaction between small groups of olivary neurons and electronic oscillators, with each subsystem thus representing a small nonlinear network of elements. By adapting techniques of modern microelectronics or nanoelectronics, it also seems feasible to compact these and related experiments to the chip scale and to consider compact integrated biological-microelectronic circuits for future applications to hybrid signal processing and computational systems that extract their usefulness from the complementary character of each subsystem.

Research supported by the BioInfoMicro Program at the U.S. Defense Advanced Research Projects Agency.

*Electronic address: Arto_Nurmikko@brown.edu

[1] D. V. R. Reddy, A. Sen, and G. L. Johnston, Phys. Rev. Lett. **85**, 3381 (2000).
[2] G. B. Ermentrout, Physica (Amsterdam) **41D**, 219 (1990).
[3] A. Szucs *et al.*, Neuroreport No. V11(N3), 2000, pp. 563–569.
[4] R. Llinas, in *Motor Control: Concepts and Issues*, edited by D. R. Humphrey and H-J. Freund (John Wiley & Sons, Berlin, 1991), p. 223; Y. Yarom and D. Cohen, Ann. N.Y. Acad. Sci. **978**, 122 (2002).
[5] M. A. Long *et al.*, J. Neurosci. **22**, 10 898 (2002).
[6] P. Varona *et al.*, Neurocomputing **44–46**, 685 (2002).
[7] C. I. De Zeeuw *et al.*, J. Neurosci. **23**, 4700 (2003).
[8] Y. Manor, J. Rinzel, I. Segev, and Y. Yarom, J. Neurophysiol. **77**, 2736 (1997).
[9] A. L. Hodgkin and A. F. Huxley, J. Physiol. **117**, 500 (1952).
[10] $I_{\text{ion}} = I_T + I_L$, where $I_T = \bar{g}_T m_\infty^3 h(V - V_{Ca})$, $I_L = g_L(V - V_L)$, and $\bar{g}_T$ the maximal calcium conductance in (mS/cm^2). $V_{Ca} = 120$ mV is the calcium reversal potential, g_L is the leak conductance, and $V_L = -63$ mV is the reversal potential of the leakage current. m_∞ is the steady-state activation (details can be found in [8]).
[11] I. Ozden and A. V. Nurmikko (unpublished).
[12] M. Lakshmanan and K. Murali, *Chaos in Nonlinear Oscillators—Control and Synchronization*, Nonlinear Science Series A Vol. 13 (World Scientific, Singapore, 1996).
[13] Y. Yarom *et al.*, Neuroscience **44**, 263 (1991).
[14] Recordings from IO cells were made in a submersion chamber filled with recording and pipette solutions used in [7]. During the experiments, the slices were at room temperature. The voltage readings from and the current coupling to the neurons were made by a patch-clamp amplifier Axoclamp 2B (Axon Instruments).
[15] Longitudinal (parasagittal) slices (300 μm thick) were prepared as described previously [5] from Sprague-Dawley rats of age P13–17. In rat brain slices, about 15% of cells on the average oscillate; for experimental convenience, we selectively chose those with the largest amplitude characteristics.
[16] R. K. Adair, Proc. Natl. Acad. Sci. U.S.A. **100**, 12 099 (2003); C. Zhou and J. Kurths, Chaos **13**, 401 (2003); J. A. White *et al.*, Trends Neurosci. **23**, 131 (2000).